

Low-energy $e^+ e^- \rightarrow \gamma \gamma$ at NNLO in QED

Tim Engel^a, Marco Rocco^b, Adrian Signer^{c,d}, and Yannick Ulrich^e

^a Kantonsschule Menzingen, 6313 Menzingen, Switzerland

^b Università degli Studi di Torino & INFN, 10125 Torino, Italy

^c PSI Center for Neutron and Muon Sciences, 5232 Villigen PSI, Switzerland

^d Physik-Institut, Universität Zürich, CH-8057 Zürich, Switzerland

^e University of Liverpool, Liverpool L69 3BX, U.K.

We present a fully differential computation of $e^+ e^- \rightarrow \gamma \gamma$ at next-to-next-to-leading order in QED. The process has been implemented into McMULE, completing its set of next-to-next-to-leading-order calculations for the most important $2 \rightarrow 2$ processes. The results allow for generic applications to electron-positron colliders with centre-of-mass energies up to a few GeV, particularly for luminosity measurements.

1 Introduction

The annihilation of an electron-positron pair into two photons, $e^+ e^- \rightarrow \gamma \gamma$, for small centre-of-mass energy, is a classical QED process. It can be used for luminosity measurements [1] and, therefore, belongs to the program of several current and future low-energy experiments [2–4]. It also plays a role as a background process in the search for dark photons [5]. Given the relevance of low-energy processes at electron-positron colliders, there has been substantial effort and progress on the theoretical side [6]. In particular, the developments concern the inclusion of hadronic effects and corrections beyond next-to-leading order (NLO) in QED.

The NLO QED corrections to $e^+ e^- \rightarrow \gamma \gamma$ have been reported long ago [7–9] but a complete and corrected result was presented only more recently [10]. Direct comparisons with experiments however require more differential calculations [11]. The current state-of-the art for fully differential cross sections is NLO+PS, provided by BabaYaga [12]. It includes the full NLO corrections combined with a resummation of collinear emission through a parton shower. While this approach does not include vacuum-polarisation (VP) contributions, their effect has been estimated in [13] for higher energies. This work also includes electroweak corrections that are relevant for higher energies, but negligible for low-energy diphoton production.

In this article, we present a fully differential calculation of $e^+ e^- \rightarrow \gamma \gamma$ at next-to-next-to-leading order (NNLO) in QED, including all photonic corrections, as well as fermion-loop corrections and dominant hadronic contributions. This calculation is complementary to the BabaYaga NLO+PS calculation. The NNLO results presented here include terms that are not included in [12], namely NNLO terms beyond the parton-shower approach. On the other hand, the NLO+PS results include terms that are not present in our calculation, namely collinear enhanced terms beyond NNLO. A comparison between the two approaches offers a possibility for mutual cross checks and a solid assessment of the theoretical uncertainties due to missing higher-order effects.

Diphoton production from a quark pair at NNLO in QCD has also received a lot of attention. Two-loop results with massive internal quarks and phenomenological results have been presented recently [14–18]. Even three-loop amplitudes with massless quarks have been considered [19]. There is, however, a crucial difference between QED and QCD calculations. In QED, the mass of the external fermions (i.e. the electrons) must not be neglected, whereas in all QCD computations, the external quarks are treated as massless. The difference originates from the fact that QED is more exclusive with respect to collinear emission.

Our calculation has been done in the MCMULE framework [20, 21], using techniques developed in the context of Bhabha [22], Møller [23], muon-electron [24], and lepton-proton [25] scattering. In particular, we use OpenLoops [26, 27] for the real-virtual corrections. The inclusion of external mass effects leads to technical complications in the two-loop amplitude. Since the corresponding massive amplitudes are not yet available, we use massified amplitudes, neglecting polynomially suppressed mass terms in the double-virtual contribution. The only additional approximation we make is to include only massless electrons for the light-by-light contributions. As we will show, these approximations are very well justified for the centre-of-mass energies $\sqrt{s} \sim \text{few GeV}$ we are interested in.

A more detailed account of the included contributions and their calculation is given in Section 2. Our results are shown in Section 3. First, we contrast our NNLO results for the total cross section with certain cuts to previous results in the literature. Next, we show differential results for experimental scenarios inspired by the KLOE and Belle II experiments. We stress that these are just illustrations. The MCMULE code can be used for generic low-energy scenarios with two detected photons. In Section 4 we present our conclusions.

2 Calculation

For the calculation of $e^+ e^- \rightarrow \gamma \gamma$ at NNLO we exploit the McMULE framework [20, 21] and follow closely the procedure used for other McMULE NNLO computations [22–25]. We write the cross section at NNLO as

$$\sigma_2 = \sigma_0 + \sigma^{(1)} + \sigma^{(2)} = \sigma_1 + \sigma^{(2)} \quad (1a)$$

$$\sigma^{(2)} = \sigma^{(2,\gamma)} + \sigma^{(2,VPe)} + \sigma^{(2,LbLe)} + \sigma^{(2,rLbLe)} \quad (1b)$$

$$\sigma^{(2+VP)} = \sigma^{(2)} + \sigma^{(2,VP\mu\tau)} + \sigma^{(2,VPh)} \quad (1c)$$

The NLO corrections $\sigma^{(1)} = \sigma^{(1,\gamma)}$ are purely photonic, i.e. there are no fermion loops. At NNLO, the corrections $\sigma^{(2)}$ are split into purely photonic contributions $\sigma^{(2,\gamma)}$, illustrated in Figure 1, and contributions with fermion loops, illustrated in Figure 2. The latter can be split further into vacuum-polarisation (VP) contributions $\sigma^{(2,VPx)}$, and light-by-light (LbL) contributions $\sigma^{(2,LbLx)}$ and $\sigma^{(2,rLbLx)}$. Here, x labels the particle in the loop and $\sigma^{(2)}$ corresponds to the NNLO corrections in QED with only electrons. Contributions from $x \neq e$ are added in $\sigma^{(2+VP)}$. The fermion-loop contributions are dominated by electron loops $x = e$, but in principle we also have to take into account other leptons $x \in \{\mu, \tau\}$, as well as hadrons $x = h$ in the loop. As we will argue below, for the low-energy scenarios we are considering here, the light-by-light contributions are strongly suppressed and it is more than sufficient to consider only electrons in the loop.

For the photonic corrections we have the usual split into double virtual (including one-loop squared), real virtual, and double real, indicated in Figure 1. As discussed in more detail in [28], for the double virtual corrections we start from the amplitudes with a massless fermion [29] and use massification [30–33]. This procedure neglects terms polynomially suppressed by the electron mass m_e . Since all four external states are well separated and we consider centre-of-mass energies $\sqrt{s} \gg m_e$, the corresponding error is completely negligible. The real-virtual amplitudes are evaluated with full mass dependence using OpenLoops [26, 27]. For the double-real contributions we use an in-house evaluation of the matrix element that was checked against OpenLoops. The loop amplitudes are renormalised in the on-shell scheme and the infrared singularities are treated with the FKS^ℓ subtraction scheme [34].

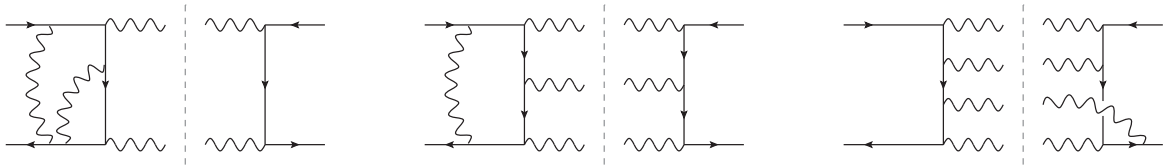


Figure 1: Representative diagrams of the squared matrix element for the double-virtual (left), real-virtual (middle), and double-real (right) contributions to the photonic corrections $\sigma^{(2,\gamma)}$.

While there are different techniques to compute the VP contributions $\sigma^{(2,VPx)}$, we found it most convenient to use a dispersive approach (for a brief overview see [6, 35]). This allows for an efficient inclusion of leptons $x \in \{e, \mu, \tau\}$ as well as hadrons $x = h$ in the loop. The latter contribution cannot be obtained using perturbation theory and we use the `alphaQED23` package [36, 37]. The two-loop VP part is separately infrared finite.

This leaves us with the light-by-light contributions that can be further split into two separately infrared-finite parts, as shown in Figure 2. The first, $\sigma^{(2,LbL)}$, consists of double-box diagrams, with one box containing the fermion (or hadron) loop. The second, $\sigma^{(2,rLbL)}$, can be considered as a real correction, as it has three photons in the final state. However, the limit of one of the photons becoming soft does not lead to a singularity. Both parts are included in our results with

a massless electron in the loop. The computation with a massive lepton loop is significantly more involved. Given the minimal numerical impact of $x \in \{\mu, \tau\}$ for the light-by-light contributions, we drop these terms. Similarly, we also do not include hadronic light-by-light contributions. Their evaluation would be even more elaborate and require techniques similar to those used for the corresponding contributions to the anomalous magnetic moment of the muon [38].

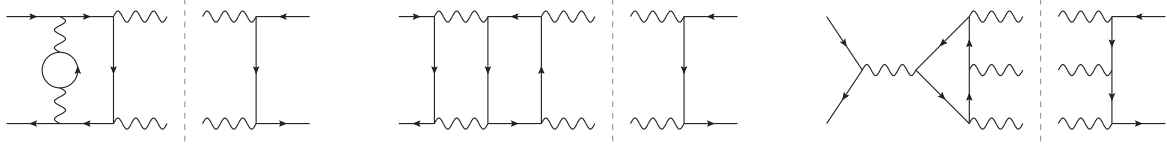


Figure 2: Representative diagrams of the squared matrix element contributing to $\sigma^{(2,VP)}$ (left), $\sigma^{(2,LbL)}$ (middle), and $\sigma^{(2,rLBL)}$ (right).

3 Results

All results presented in the following are publicly available in the MCMULE user library [39]

<https://mule-tools.gitlab.io/user-library/diphoton/nnlo-studies>

3.1 Total cross sections

We have compared the NLO total cross section without any cuts to the analytic results given in [10]. For very low energies $\sqrt{s} \lesssim 10$ MeV it is straightforward to obtain Monte Carlo errors of 10^{-6} , whereas for energies approaching $\sqrt{s} \simeq 10$ GeV the Monte Carlo errors increase to 10^{-4} . In all cases we have found agreement within these errors.

We start the presentation of our NNLO results with the total cross section for three values of $\sqrt{s} \in \{1, 3, 10\}$ GeV. In addition we apply the following cuts

$$\theta_\gamma^{\min} = 45^\circ, \quad \theta_\gamma^{\max} = 135^\circ, \quad (2a)$$

$$E_\gamma^{\min} = 0.3 \sqrt{s}, \quad \xi^{\max} = 10^\circ. \quad (2b)$$

Thus, we request at least two photons with energy larger than E_γ^{\min} in an angular range determined by θ_γ^{\min} and θ_γ^{\max} . The acollinearity $\xi \equiv |\theta_+ + \theta_- - 180^\circ|$ of the two most energetic photons satisfying these cuts must be smaller than ξ^{\max} . These cuts correspond precisely to cuts used in [12], with the results reported in [1].

Our results are summarised in Table 1 and compared to [12]. The NLO results agree within 0.01% and the corrections are between 6 – 8%. Beyond NLO, there are physical differences between [12] and our results. We have included the full $\mathcal{O}(\alpha^2)$ NNLO corrections, whereas in [12] photonic corrections beyond NLO have been implemented with a parton-shower approach. Thus, VP, LbL, and some non-logarithmic $\mathcal{O}(\alpha^2)$ corrections are missing in [12]. On the other hand, they resum the leading-logarithmic corrections from multiple photon emission and, hence, include dominant terms of photonic corrections also beyond NNLO. Rather than comparing the best predictions it is thus more informative to compare the exact photonic NNLO corrections $\sigma^{(2,\gamma)}$ with the parton-shower induced contributions beyond NLO. In the notation of [12], where $\sigma_\alpha^{\text{NLO}}$ is used for σ_1 , they are given by $\sigma_{\text{exp}} - \sigma_1$. As can be seen from Table 1, the two approaches agree within 10 – 20% and give beyond-NLO photonic corrections of the order of 0.2 – 0.5%. Taking into account the $\mathcal{O}(\alpha^2)$ suppression, this results in differences of the order of 0.05%.

In McMULE also further NNLO corrections are included. In particular, there are VP corrections due to an electron loop, $\sigma^{(2,VPe)}$. These corrections are negative and about 20% of $\sigma^{(2,\gamma)}$, becoming slightly more important for increasing \sqrt{s} . Including $\sigma^{(2,VPe)}$ in the McMULE result leads to near-perfect agreement with the parton-shower result, but this agreement is accidental. The VP corrections with heavier particles in the loop, $\sigma^{(2,VP\mu\tau)}$ and $\sigma^{(2,VPh)}$, are strongly suppressed for the small centre-of-mass energies considered here. Even for $\sqrt{s} = 10$ GeV they are about a factor 100 smaller than $\sigma^{(2,VPe)}$. Thus, they can be safely neglected. In fact, they are smaller than the numerical differences of the NLO results. This also holds for light-by-light contributions with an electron in the loop, $\sigma^{(2,LbLe)}$ and $\sigma^{(2,rLbLe)}$. These results fully justify the neglect of the corresponding contributions with heavier leptons or hadrons in the loop.

\sqrt{s}	1 GeV		3 GeV		10 GeV	
	McMULE [nb]	[12] [nb]	McMULE [nb]	[12] [nb]	McMULE [nb]	[12] [nb]
σ_0	137.531	137.53	15.2812	15.281	1.37531	1.3753
σ_1	129.444	129.45	14.2099	14.211	1.26185	1.2620
σ_2	129.760		14.2570		1.26738	
σ_{exp}		129.77		14.263		1.2685
$\sigma^{(2,\gamma)}$	0.383		0.0598		0.00738	
$\sigma_{\text{exp}} - \sigma_1$		0.32		0.053		0.0065
$\sigma^{(2,VPe)}$	-0.069		-0.0128		-0.00186	
$\sigma^{(2,LbLe)}$	-0.0014		-0.00016		-0.000014	
$\sigma^{(2,rLbLe)}$	0.0030		0.00033		0.000030	
$\sigma^{(2,VP\mu\tau)}$	-0.000077		-0.00018		-0.000080	
$\sigma^{(2,VPh)}$	0.000090		-0.00010		-0.000097	

Table 1: Different contributions to the NNLO cross section computed by McMULE and compared to results in [12]. Regarding the latter, σ_{exp} corresponds to matching a complete NLO result with a parton-shower resummation.

To summarise the situation for the total cross section we confirm the estimate of the theoretical accuracy of 0.1% given in [12]. We continue the presentation of our results with differential distributions in two different scenarios, inspired by the KLOE and BELLE II experiments.

3.2 Differential cross sections for a KLOE-like scenario

The centre-of-mass energy is set to $\sqrt{s} = 1.0$ GeV and we require at least two photons with

$$E_\gamma \geq 300 \text{ MeV} \quad \text{and} \quad 45^\circ \leq \theta_\gamma \leq 135^\circ. \quad (3)$$

In addition we apply the cut on the acollinearity, requiring

$$\xi \equiv |\theta_l + \theta_s - \pi| \leq 10^\circ, \quad (4)$$

where θ_l and θ_s are the angles of the two most energetic photons satisfying (3). We apply a beam spread for both incoming particles, with a Gaussian distribution of FWHM 0.12 MeV [40]. A beam spread is able to cure largely fluctuating distributions caused by soft enhancements when the energies of tree-level photons are equal. Further, the sorting algorithm for photons in the final state requires a percent-level energy resolution, otherwise the event is randomly ordered.

The differential distribution with respect to

$$\theta_{av} \equiv \frac{1}{2}(\theta_l - \theta_s + \pi) \quad (5)$$

is shown in Figure 3. The symmetrical shape is due to the symmetrical beam energies. NNLO corrections amount to a few permille, with strong enhancements at the edges of the distribution, up to 2%. The lower panel confirms the negligibility of non-photonic corrections compared to photonic corrections, particularly for this low-energy KLOE-like scenario. The by-far biggest contribution among non-photonic corrections is due to $\sigma^{(2,VPe)}$, i.e. diagrams with an electronic vacuum polarisation insertion. While these are computed with no approximations, $\sigma^{(2,LbLe)}$ and $\sigma^{(2,rLbLe)}$ are computed for electronic insertions only, further with a massless electron. The size of the latter corrections justifies the approximation, hence the allusion in Section 2.

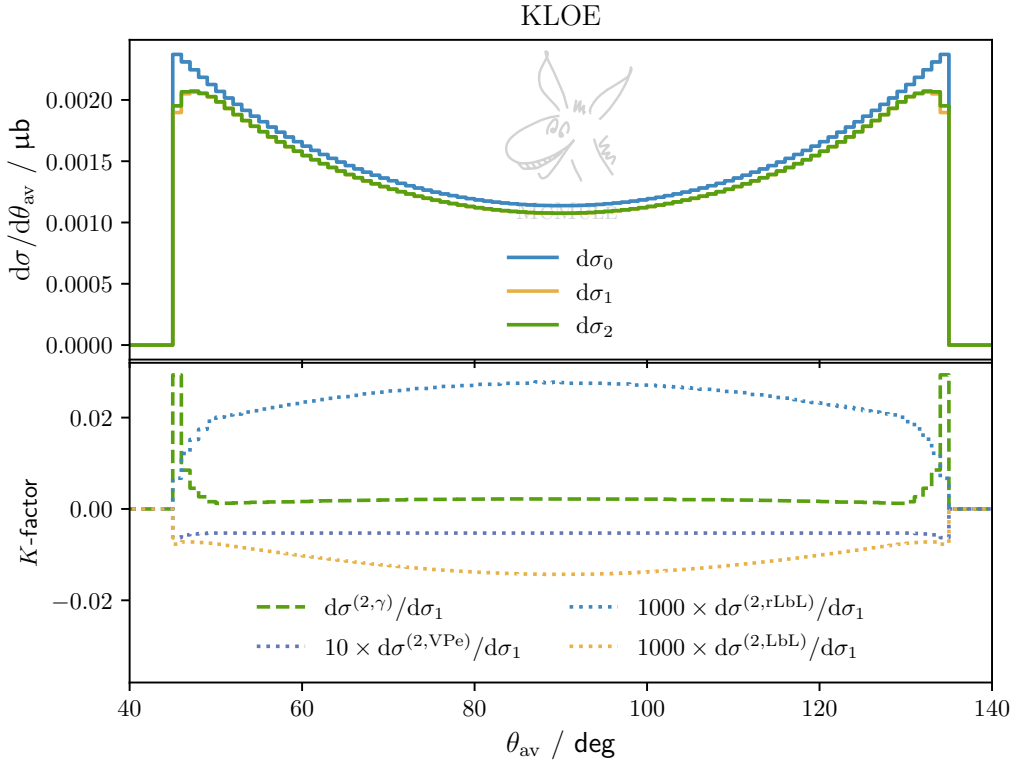


Figure 3: Differential distribution with respect to θ_{av} for the KLOE-like scenario. The blue, orange, and green curves in the upper panel correspond to LO-, NLO-, and NNLO-precise distributions, respectively. The size of NNLO photonic and non-photonic corrections are presented in the lower panel with respect to the NLO distribution, with varying enhancing factors for the latter.

3.3 Differential cross sections for a Belle-like scenario

The process is $e^-(7 \text{ GeV}) e^+(4 \text{ GeV}) \rightarrow \gamma \gamma$ with at least two photons satisfying

$$E_\gamma \geq 1 \text{ GeV} \quad \text{and} \quad 15^\circ \leq \theta_\gamma \leq 165^\circ. \quad (6)$$

Even though we use a symmetric angular cut, the parameters of the photons are understood to be in the LAB frame. Hence, photons tend to be emitted forward, i.e. $\theta_\gamma > 90^\circ$. The centre-of-mass

energy is $\sqrt{s} = 10.583$ GeV. No beam spread is applied in this case, as the beam energies are asymmetrical by construction.

The differential distribution with respect to θ_{av} is presented for this scenario as well, and is shown in Figure 4. NNLO corrections amount to a few permille, with enhancements below $\sim 85^\circ$ and above $\sim 160^\circ$, where the LO contribution is zero and the NNLO calculation effectively provides an NLO result. The size of non-photonic corrections is larger than in the KLOE-like scenario, due to the higher centre-of-mass energy. The biggest contribution among non-photonic corrections is due to $\sigma^{(2,VPe)}$, i.e. diagrams with an electronic vacuum polarisation insertion, whose size grows at higher energies. This term is of the order of 0.1%, so should be included according to the accuracy goal. Instead, $\sigma^{(2,LbLe)}$ and $\sigma^{(2,rLbLe)}$, as well as contributions with heavier particles in the loop, require large enhancing factors in order to become visible on the plot.

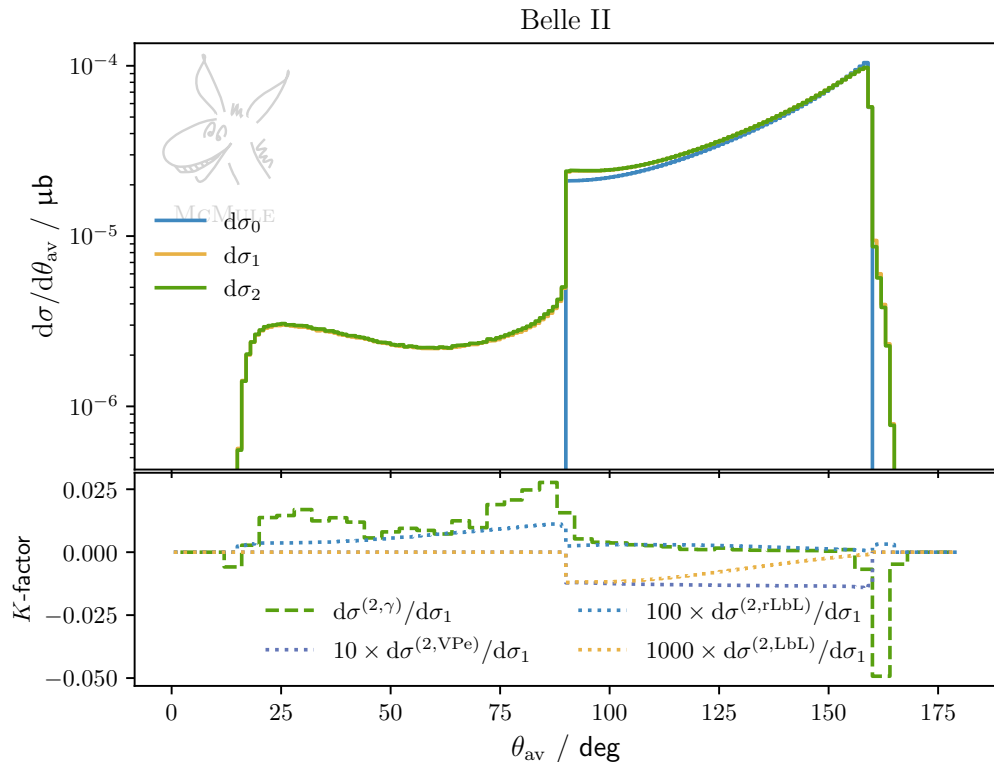


Figure 4: Differential distribution with respect to θ_{av} for the Belle-like scenario. The blue, orange, and green curves in the upper panel correspond to LO-, NLO-, and NNLO-precise distributions, respectively. The size of NNLO photonic and non-photonic corrections are presented in the lower panel with respect to the NLO distribution, with varying enhancing factors for the latter.

4 Conclusion

We have presented a complete NNLO QED calculation for photon pair production at low-energy electron-positron colliders. The results have been implemented into McMULE and as an illustration we have shown distributions for scenarios inspired by the KLOE and Belle experiments. However, we stress that the code allows the computation of any differential cross section with arbitrary (infrared-safe) cuts. Since the computation is pure QED, the centre-of-mass energy has

to be sufficiently small to justify the neglect of electroweak effects.

This calculation is based on techniques developed in the context of previous McMULE NNLO computations. It completes the set of fully differential NNLO calculations for the most important $2 \rightarrow 2$ processes in McMULE. From the current results it is in principle also possible to obtain Compton scattering at NNLO through crossing.

The comparison of the photonic NNLO calculation of $e^+ e^- \rightarrow \gamma \gamma$ to previous NLO+PS results confirms earlier error estimates of the order of 0.1%. The fermionic corrections are of a similar size. This is a clear indication that terms beyond NNLO as well as the terms beyond NLO+PS have an impact at most at the permille level. This comparison is indeed one of the most reliable ways to estimate the effect of missing higher-order corrections. It will be very interesting to perform a similar comparison for $2 \rightarrow 3$ processes. With the available techniques, there are no decisive obstacles towards this goal.

Acknowledgements

It is a pleasure to thank Luca Naterop for his contributions at the initial stage of this project. We would like to thank Carlo Carloni Calame and Fulvio Piccinini for discussions regarding the comparison of our NNLO results to their NLO+PS results, and Graziano Venanzoni for explanations regarding the beam-energy spread at KLOE. We acknowledge support by the Swiss National Science Foundation (SNSF) under grant 207386, and by the Italian Ministry of Universities and Research (MUR) through grants PRIN 2022BCXSW9 and FIS (CUP: D53C24005480001, FLAME).

References

- [1] WORKING GROUP ON RADIATIVE CORRECTIONS, MONTE CARLO GENERATORS FOR LOW ENERGIES collaboration, S. Actis et al., *Quest for precision in hadronic cross sections at low energy: Monte Carlo tools vs. experimental data*, *Eur. Phys. J. C* **66** (2010) 585 [[0912.0749](#)].
- [2] BELLE-II collaboration, W. Altmannshofer et al., *The Belle II Physics Book*, *PTEP* **2019** (2019) 123C01 [[1808.10567](#)].
- [3] BESIII collaboration, M. Ablikim et al., *Luminosity measurements for the R scan experiment at BESIII*, *Chin. Phys. C* **41** (2017) 063001 [[1702.04977](#)].
- [4] BESIII collaboration, M. Ablikim et al., *Luminosities and energies of e^+e^- collision data taken between $\sqrt{s} = 4.61$ GeV and 4.95 GeV at BESIII*, *Chin. Phys. C* **46** (2022) 113003 [[2205.04809](#)].
- [5] M. Raggi and V. Kozhuharov, *Proposal to Search for a Dark Photon in Positron on Target Collisions at DAΦNE Linac*, *Adv. High Energy Phys.* **2014** (2014) 959802 [[1403.3041](#)].
- [6] RADIOMONTECARLOW 2 collaboration, R. Aliberti et al., *Radiative corrections and Monte Carlo tools for low-energy hadronic cross sections in e^+e^- collisions*, *SciPost Phys. Comm. Rep.* **2025** (2025) 9 [[2410.22882](#)].
- [7] G. Andreassi, G. Calucci, G. Furlan, G. Peressutti and P. Cazzola, *Radiative corrections to the total cross section for annihilation of a pair into photons*, *Phys. Rev.* **128** (1962) 1425.
- [8] S. I. Eidelman and E. A. Kuraev, *$e^+ e^-$ Annihilation Into Two and Three Photons at High-Energy*, *Nucl. Phys. B* **143** (1978) 353.

[9] F. A. Berends and R. Kleiss, *Distributions for Electron-Positron Annihilation Into Two and Three Photons*, *Nucl. Phys. B* **186** (1981) 22.

[10] R. N. Lee, *Electron-positron annihilation to photons at $O(\alpha^3)$ revisited*, *Nucl. Phys. B* **960** (2020) 115200 [[2006.11082](#)].

[11] A. B. Arbuzov, G. V. Fedotovich, E. A. Kuraev, N. P. Merenkov, V. D. Rushai and L. Trentadue, *Large angle QED processes at e^+e^- colliders at energies below 3-GeV*, *JHEP* **10** (1997) 001 [[hep-ph/9702262](#)].

[12] G. Balossini, C. Bignamini, C. M. C. Calame, G. Montagna, O. Nicrosini and F. Piccinini, *Photon pair production at flavour factories with per mille accuracy*, *Phys. Lett. B* **663** (2008) 209 [[0801.3360](#)].

[13] C. M. Carloni Calame, M. Chiesa, G. Montagna, O. Nicrosini and F. Piccinini, *Electroweak corrections to $e^+e^- \rightarrow \gamma\gamma$ as a luminosity process at FCC-ee*, *Phys. Lett. B* **798** (2019) 134976 [[1906.08056](#)].

[14] M. Becchetti, R. Bonciani, L. Cieri, F. Coro and F. Ripani, *Full top-quark mass dependence in diphoton production at NNLO in QCD*, *Phys. Lett. B* **848** (2024) 138362 [[2308.10885](#)].

[15] M. Becchetti, R. Bonciani, L. Cieri, F. Coro and F. Ripani, *Two-loop form factors for diphoton production in quark annihilation channel with heavy quark mass dependence*, *JHEP* **12** (2023) 105 [[2308.11412](#)].

[16] M. Becchetti, F. Coro, C. Nega, L. Tancredi and F. J. Wagner, *Analytic two-loop amplitudes for $q\bar{q} \rightarrow \gamma\gamma$ and $gg \rightarrow \gamma\gamma$ mediated by a heavy-quark loop*, *JHEP* **06** (2025) 033 [[2502.00118](#)].

[17] T. Ahmed, A. Chakraborty, E. Chaubey and M. Kaur, *Two-loop helicity amplitudes for diphoton production with massive quark loop*, [2502.03282](#).

[18] F. Coro, *Full NNLO QCD corrections to diphoton production*, *PoS EPS-HEP2023* (2024) 263 [[2310.10458](#)].

[19] F. Caola, A. Von Manteuffel and L. Tancredi, *Diphoton Amplitudes in Three-Loop Quantum Chromodynamics*, *Phys. Rev. Lett.* **126** (2021) 112004 [[2011.13946](#)].

[20] P. Banerjee, T. Engel, A. Signer and Y. Ulrich, *QED at NNLO with McMule*, *SciPost Phys.* **9** (2020) 027 [[2007.01654](#)].

[21] Y. Ulrich, *McMule – QED Corrections for Low-Energy Experiments*, Ph.D. thesis, University of Zurich, Aug, 2020. [2008.09383](#).

[22] P. Banerjee, T. Engel, N. Schalch, A. Signer and Y. Ulrich, *Bhabha scattering at NNLO with next-to-soft stabilisation*, *Phys. Lett. B* **820** (2021) 136547 [[2106.07469](#)].

[23] P. Banerjee, T. Engel, N. Schalch, A. Signer and Y. Ulrich, *Møller scattering at NNLO*, *Phys. Rev. D* **105** (2022) L031904 [[2107.12311](#)].

[24] A. Broggio et al., *Muon-electron scattering at NNLO*, *JHEP* **01** (2023) 112 [[2212.06481](#)].

[25] T. Engel, F. Hagelstein, M. Rocco, V. Sharkovska, A. Signer and Y. Ulrich, *Impact of NNLO QED corrections on lepton-proton scattering at MUSE*, *Eur. Phys. J. A* **59** (2023) 253 [[2307.16831](#)].

[26] F. Buccioni, S. Pozzorini and M. Zoller, *On-the-fly reduction of open loops*, *Eur. Phys. J. C* **78** (2018) 70 [[1710.11452](https://arxiv.org/abs/1710.11452)].

[27] F. Buccioni, J.-N. Lang, J. M. Lindert, P. Maierhöfer, S. Pozzorini, H. Zhang et al., *OpenLoops 2*, *Eur. Phys. J. C* **79** (2019) 866 [[1907.13071](https://arxiv.org/abs/1907.13071)].

[28] L. Naterop, “Electron positron annihilation into photons at NNLO accuracy.” Master’s thesis, University of Zurich, https://mule-tools.gitlab.io/_static/LN-msc.pdf, 2021.

[29] C. Anastasiou, E. W. N. Glover and M. E. Tejeda-Yeomans, *Two loop QED and QCD corrections to massless fermion boson scattering*, *Nucl. Phys. B* **629** (2002) 255 [[hep-ph/0201274](https://arxiv.org/abs/hep-ph/0201274)].

[30] A. A. Penin, *Two-loop photonic corrections to massive Bhabha scattering*, *Nucl. Phys. B* **734** (2006) 185 [[hep-ph/0508127](https://arxiv.org/abs/hep-ph/0508127)].

[31] T. Becher and K. Melnikov, *Two-loop QED corrections to Bhabha scattering*, *JHEP* **06** (2007) 084 [[0704.3582](https://arxiv.org/abs/0704.3582)].

[32] A. Mitov and S. Moch, *The Singular behavior of massive QCD amplitudes*, *JHEP* **05** (2007) 001 [[hep-ph/0612149](https://arxiv.org/abs/hep-ph/0612149)].

[33] T. Engel, C. Gnendiger, A. Signer and Y. Ulrich, *Small-mass effects in heavy-to-light form factors*, *JHEP* **02** (2019) 118 [[1811.06461](https://arxiv.org/abs/1811.06461)].

[34] T. Engel, A. Signer and Y. Ulrich, *A subtraction scheme for massive QED*, *JHEP* **01** (2020) 085 [[1909.10244](https://arxiv.org/abs/1909.10244)].

[35] Y. Fang, S. Kollatzsch, M. Rocco, A. Signer, Y. Ulrich and M. Zoller, *Disperon QED*, [2512.10709](https://arxiv.org/abs/2512.10709).

[36] F. Jegerlehner, *Precision measurements of σ_{hadronic} for $\alpha_{\text{eff}}(E)$ at ILC energies and $(g-2)_\mu$* , *Nucl. Phys. B Proc. Suppl.* **162** (2006) 22 [[hep-ph/0608329](https://arxiv.org/abs/hep-ph/0608329)].

[37] F. Jegerlehner, “Software packages alphaQED and pQCDAdler.” <http://www-com.physik.hu-berlin.de/~fjeger/software.html>, 2023.

[38] R. Aliberti et al., *The anomalous magnetic moment of the muon in the Standard Model: an update*, [2505.21476](https://arxiv.org/abs/2505.21476).

[39] McMULE Team, “McMULE dataset.” <https://doi.org/10.5281/zenodo.8188752>.

[40] KLOE collaboration, F. Ambrosino et al., *Measurement of the leptonic decay widths of the phi-meson with the KLOE detector*, *Phys. Lett. B* **608** (2005) 199 [[hep-ex/0411082](https://arxiv.org/abs/hep-ex/0411082)].